Available online at www.sciencedirect.com
SCIENCE DIRECT®
Continental Shelf Research 24 (2004) 241–262
CONTINENTAL SHELF RESEARCH
www.elsevier.com/locate/csr

Lagrangian and satellite observations of the Brazilian Coastal Current

Ronald Buss de Souza[a,*], Ian S. Robinson[b]

[a] *Remote Sensing Division, National Institute for Space Research, Av. dos Astronautas 1758, São José dos Campos, SP 12227-010, Brazil*
[b] *Southampton Oceanography Centre, School of Ocean and Earth Science, University of Southampton, European Way SO14 3ZH, UK*

Accepted 1 October 2003

Abstract

The waters dominating the Brazilian Continental Shelf to the south of Santa Marta Cape (28°40′S) are marked by their strong interannual variability. Both the seasonal oscillation of the Brazil–Malvinas (Falkland) Confluence (BMC) region and the seasonal variations of the La Plata River and Patos Lagoon outflows are reflected in the seasonal changes of the vertical and horizontal water mass structure in the Southern Brazilian Shelf. In the region to the north of Santa Marta Cape, the shelf is mainly described in the literature as dominated by Tropical Waters (TW) transported southwards by the Brazil Current (BC). However, the first Lagrangian (buoy) measurements made on the inner Brazilian shelf have shown that a coastal current flowing in the opposite direction in relation to the BC occurred on the shelf as far north as 24°S during the 1993 austral autumn and winter. Recent papers have suggested that the arrival at low latitudes of cold waters originating in the BMC region is an anomalous phenomenon and that it can be either forced by local winds during wintertime or related to the ENSO. High-resolution sea surface temperature (SST) imagery and the Lagrangian measurements taken in 1993 and 1994 are used in this paper to describe the temperatures, velocity, energy and oscillations present in this coastal current. These two data sets show that the current is not only fed by waters of Subantarctic or coastal origin but also receives a contribution of TW at the surface by lateral mixing. By analysing a set of monthly averaged SST images from 1982 to 1995, this work suggests that the intrusion of cold waters transported by the coastal current can be a regular winter phenomenon occurring on the Brazilian shelf at latitudes up to the vicinity of 25°S. Given its consistency, this current is named here the Brazilian Coastal Current.

Keywords: South-western Atlantic; Southern Brazilian Shelf; Surface currents; Drifting buoys; AVHRR; COROAS; WOCE

1. Introduction

1.1. Water masses and their seasonal behaviour in the South-western Atlantic

The hydrography of the Brazilian Continental Shelf waters, in the South-western Atlantic Ocean

*Corresponding author. Tel.: +55-12-3945-6504; fax: +55-12-3945-6488.
E-mail address: ronald@dsr.inpe.br (R.B. de Souza).

0278-4343/$ - see front matter © 2003 Elsevier Ltd. All rights reserved.
doi:10.1016/j.csr.2003.10.001

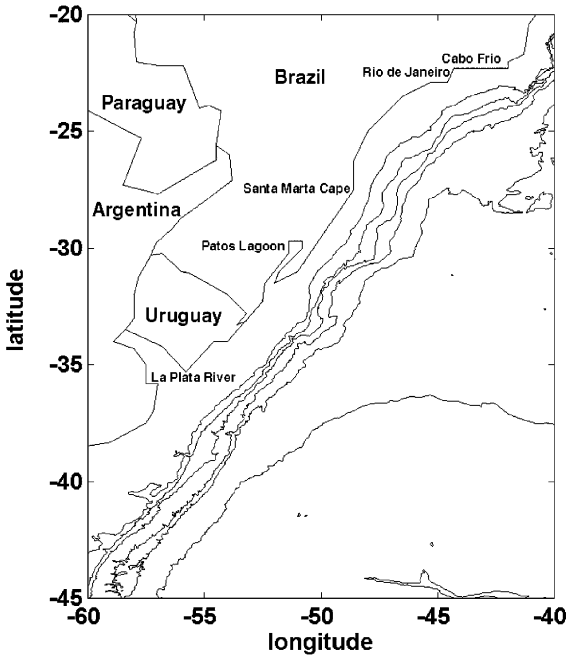

Fig. 1. South-western Atlantic Ocean with its main features. The 100, 200, 1000, 2000, 3000, 4000 and 5000 m isobaths are shown.

(Fig. 1), was first studied by the pioneering works of Emílsson (1959, 1961), who extended the understanding of the water mass characteristics of the South Atlantic Ocean made earlier by Defant (1936) and Sverdrup et al. (1942). The surface circulation regime of the South Atlantic Ocean, as summarised by Peterson and Stramma (1991) and Stramma and England (1999), presents an anticyclonic gyre in which the Brazil Current (BC) represents the western boundary current.

The water mass structure in the South-western Atlantic Ocean (SWA hereafter) is complex, especially in the region where BC meets the equatorward Malvinas (Falkland) Current (MC). This region, known as the Brazil–Malvinas Confluence (BMC), is considered one of the most complex regions of the world ocean. Longhurst (1998) points out that a total of seven different subsurface water masses can be found at the BMC, with their origins in the North Atlantic, South Pacific, Southern Ocean and in the BMC itself. At the surface, BC carries Tropical Water (TW) and MC carries the cooler and fresher Subantarctic Water (SAW).

The thermohaline limits for the water masses present in the SWA are described by various authors (e.g. Emílsson, 1961; Thomsen, 1962; Miranda, 1972, 1982; Castro and Miranda, 1998). Although small variations are accepted for some of the other water masses, the thermohaline limits for TW are, in most cases, fixed at $T > 20^{\circ}C$ and $S > 36$.

Although very few direct measurements have been made in the past to characterise the BC, MC and the currents occurring in the Brazilian shelf, hydrography and satellite images have indicated the presence of distinct surface water masses and of strong lateral gradients between them. In most works the 20°C isotherm is generally interpreted as the limit between the water masses carried by the BC and the MC at the surface (e.g. Sunyé, 1999). Souza (2000) has also demonstrated that BC/MC and BC/Coastal waters (CW) horizontal thermal gradients are about 0.1°C/km having in most cases the 20°C isotherm embedded in them.

The mean latitudes where the BC meets the MC in the BMC region are between 36°S and 39°S (Reid et al., 1977), depending on the season of the year. As the western extreme of the Subtropical Front (STF), the oscillation of the BMC region is directly linked to the oscillation of the front. Along the STF, as well as in the BMC region, the mixing between TW and SAW produces the South Atlantic Central Water (SACW). This water mass recirculates in the South Atlantic and is also transported by the BC to the south below the superficial TW (Garfield, 1990).

Continental runoff, particularly that from the La Plata River (36°S, 56°W) and from the Patos Lagoon (32°S, 52°W), contributes to make the horizontal and vertical structure of the BMC region even more complex, with the addition of CW. The same applies to the region of the Southern Brazilian Continental Shelf (SBCS).[1] A water mass classification made by Castro and

[1] SBCS in this text denotes the regions named by Castro and Miranda (1998) as Southern Brazilian Shelf (from Arroio Chuí—33°48′S to Santa Marta Cape—28°40′S) and SBB (from Santa Marta Cape to Cabo Frio—23°S).

Miranda (1998) describes two kinds of CW occurring at the SBCS: CW influenced by SAW ($S<34$) and CW influenced by TW or Shelf Break Water ($34<S<36.7$). A more recent and complete classification made by Piola et al. (2000) for the South American coast between 20°S and 40°S had also identified two water masses in the region: (a) the Subantarctic Shelf Water (SASW) and (b) the Subtropical Shelf Water (STSW). The later is formed by the dilution of SACW by continental runoff from the coast of Brazil.

The thermohaline characteristics of the SBCS waters are highly seasonal. As far as it is known, this seasonal behaviour is related to changes in the local wind regime and in the continental freshwater discharge, especially that of the La Plata River and Patos Lagoon (Miranda, 1972; Garcia, 1997; Castro and Miranda, 1998). Associated with the seasonal changes in the water masses at the SBCS, the wintertime shelf waters off Southern Brazil are supposed to be exposed to a coastal current coming from the BMC region. In the shelf off Argentina, a coastal current is known to exist travelling parallel to the MC flow (Piola and Rivas, 1997; Piola et al., 2000). The waters carried by this current are fresher than those of the MC, and the nature of the flow resulting from the interaction of this current with the La Plata River discharge waters is still object of investigation. Climatological means of the sea surface temperature (SST) and salinity fields presented by Zavialov et al. (1999) indicate that the current displacing cold and fresh waters coming from Argentina is also present over the SBCS in wintertime.

Piola et al. (2000) reported that the STSW suffers substantial dilution at the surface layer by the continental runoff of the La Plata River and Patos Lagoon. The resulting outflow forms a low-salinity tongue that covers the shelf water and extends northwards over the shelf, penetrating lower latitudes in wintertime. E.J.D. Campos (pers. comm.), however, points out to the fact that any northwards current associated to this low-salinity tongue would, necessarily, be restricted to the first 50 m depth waters.

Given the absence of consistent direct measurements of currents in the southern part of the SBCS, Zavialov et al. (1998) developed an inverse model based upon historical hydrographic and meteorological data to study the currents in that region. They concluded that a northwards current must occur all the year long at the shelf in the area between 30°S and 35°S. Zavialov et al. (1999) add that the shelf break off Southern Brazil and Uruguay is (in words) 'virtually the line of no motion' separating the BC flowing southwards along the continental slope and the northwards flow on the shelf.

Nevertheless, Guerrero et al. (1997) studied the La Plata River estuary and concluded that a northwards drift of fresher waters originating in the estuary only happens in wintertime, under a condition of balance between onshore and offshore winds, and under higher continental drainage. They considered a line perpendicular to the axis of the La Plata River, and divided wind data into onshore (from NE, E, SE and S) and offshore (from NW, W, SW and N) components. Onshore winds act to pile up water in the La Plata estuary while offshore winds increase seaward discharge.

Guerrero et al. (1997) also reported that the monthly mean discharge of the La Plata River is higher (about 25,000 m^3/s) during the months of April–July, reducing to about 20,000 m^3/s in the rest of the year. Water outflow from the La Plata River is deflected to the north by Coriolis force when entering the continental shelf. The flow generated at the shelf from La Plata River is considered to be barotropic and geostrophic, being driven by the sea surface elevation. This latter is caused by the river discharge and Ekman transport (Zavialov et al., 1998).

$T-S$ diagrams for the SBCS and farther south are presented by Odebrecht and Garcia (1997), Castro and Miranda (1998) and Piola et al. (2000). The diagrams show that the CWs in the SBCS region change their thermohaline characteristics seasonally, reaching very low-salinity limits in spring and winter. Odebrecht and Garcia (1997), for instance, found salinity as low as 26 during spring. Values of the same magnitude were also found for the region of influence of the La Plata River, in Argentina, during summertime (Guerrero and Piola, 1997). Castro and Miranda (1998) also indicate that there is a discontinuity of $T-S$

points between CW and SACW in winter at the SBCS. This implies minimal or non-existent mixing between these two water masses in wintertime. The same is valid for the relation between SASW and STSW described by Piola et al. (2000).

The Odebrecht and Garcia (1997) work also reports that the distinct water masses of the SBCS have different chlorophyll patterns. CW and SAW are considered eutrophic waters, with higher chlorophyll content than the TW (Ciotti et al., 1995). The presence of these waters, therefore, is important for the entire trophic system. Since a coastal current flowing northwards would carry eutrophic waters from the south to the SBCS, the investigation of this current is very important for assessing the changing biological characteristics of this area.

1.2. Currents in the South Brazilian Continental Shelf

During wintertime, CW dominates the inner SBCS and is reported to reach maximum latitudes of 28°S at Santa Marta Cape (Campos et al., 1996a) or 27°S at Santa Catarina Island (Piccolo, 1998). Although the shape of the isotherms derived from hydrographic surveys in the SBCS suggests an advection of the CW to the north, very few direct measurements of currents have so far been made in the SBCS or in the Brazilian part of the BMC region. Although Zavialov et al. (1998) modelled the northwards coastal current occurring in the SBCS up to 30°S, no previous work has explicitly sought to find a general understanding of the propagation limits of this current over the SBCS throughout the year.

During 1985, three inverted echo-sounders were deployed in the BMC at about 37.5°S by Garzoli and Garraffo (1989), and Pegasus measurements were made at 24°S and 31°S by Garfield (1990). Castro and Miranda (1998) also reported some other measurements made by them and others in the South Brazil Bight (SBB, 24–28°S). The last authors added that the local south-westerly or north-easterly winds drive the inner shelf currents to follow their directions in a bimodal distribution during all seasons of the year.

The first direct current meter measurements made on the continental shelf of Southern Brazil are described by Zavialov and Möller (2000) and Zavialov et al. (2002). The authors have deployed two current meters at 15 and 40 m depth in a mooring station at 32°41′S–51°27′W during the period from March to August 1997. The results of the current velocity time series confirmed model results presented earlier by Zavialov et al. (1998), suggesting a northwards current at the Brazilian Continental Shelf. Zavialov and Möller (2000) described the so-called 'Rio Grande Current' as strongly barotropic and related to the La Plata and Patos Lagoon freshwater discharges. They also pointed out that the coastal current flow is often seen in satellite imagery and occupies the entire shelf extending to about 27°S or even farther north. Along-shore mean velocity (from a 151 days long time series) for the 15 m current studied by Zavialov et al. (2002) was 1.8 cm/s towards the north-east. However, extreme speeds reached about 100 cm/s and current reversals were registered at periods close to 10 days.

1.3. Brazilian counterpart to WOCE

The conception of a local counterpart for the World Ocean Circulation Experiment (WOCE) by Brazilian oceanographers in 1992 aimed to remedy the lack of knowledge about the ecological aspects of the SBB and nearby areas of the Brazil Basin in the SWA (Campos et al., 1996b). Project COROAS (Oceanic Circulation in the Western Region of the South Atlantic) was a multi-disciplinary program which included hydrographic surveys, Lagrangian and Eulerian measurements of currents, space oceanography and biological and chemical sampling off the Brazilian coast. For the first time in Brazilian oceanography, a series of consistent high-resolution infrared satellite images was recorded over the coast for a period of over 2 years together with the deployment of surface drifters in the BC.

One of the new facts that came to light after the experimental phase of COROAS is that low-salinity, cold waters carried by a so-named 'coastal branch of the MC' (erroneously named as, because of potential vorticity requirements of the MC, this

current is unlikely to penetrate the continental shelf; O.O. Möller Jr., pers. comm.) or 'waters coming from the BMC region' were found to reach latitudes of about 24°S, near Rio de Janeiro city (Stevenson and Souza, 1994; Stevenson, 1996; Campos et al., 1996a, b, 1999; Silva Jr. et al., 1996). Owing to the limited time series of satellite images collected through COROAS (only 2 years long), however, the intrusion of cold CW in latitudes north of 28°S was supposed to be an anomalous process.

Using COROAS and other sources of data, Stevenson et al. (1998) studied the ecological aspects of the tropical Ilha Grande Bay (22°S), off Rio de Janeiro State, Brazil. These authors suggested that Subantactic organisms present there have been carried along the SBCS by the coastal current coming from the south. However, they still considered that the entrance of Subantarctic biota to Ilha Grande Bay happens in a sporadic way. The authors cited the passage of meteorological fronts through the SBCS as an important, if not the principal, driving mechanism for carrying waters with Subantarctic origin to the north.

1.4. Objectives

It is the clarification of the winter behaviour of the intrusion of cold waters in the SBCS which provides the motivation for this paper. In particular, we wish to analyse further the character of the supposed anomalous behaviour, since it could be of considerable significance for the productivity and the economical aspects of the area. Ciotti et al. (1995) point out that the southern part of the Brazilian Continental Shelf is the most important fishery area of the Brazilian coast. High phytoplankton biomass is related to nutrients made available from the intrusion of SAW and CW on the shelf. The possibility of an extension of the most productive fishery area of the Brazilian shelf to the north of 28°S is surely of enormous economical importance in Brazil.

Lagrangian (buoy) data collected during COROAS are analysed in detail to describe the temperatures, velocities, energies and oscillations of the coastal current present in the SBCS. High-resolution Advanced Very High-Resolution Radiometer (AVHRR) data are used to show the interactions between the BC and the coastal current at the surface. Low-resolution images of the South Atlantic Ocean are analysed for the period of January 1982–December 1995 to demonstrate that the intrusion of cold waters up to latitudes near 24°S could be not an anomalous phenomenon, but rather a common process occurring in the SBCS during wintertime.

2. Data and methods

2.1. Drifters

Project COROAS has provided the first opportunity for a Lagrangian description of the Brazilian continental waters. The COROAS surface floats consisted of Low Cost Drifters (LCDs) drogued at 15 m depth, following the WOCE standard design proposed by Sybrandy and Niiler (1991). Data transmission was done via ARGOS Service. SST was measured by the LCDs during the buoy's advection on the surface, at 12 cm beneath the water line with an accuracy of 0.12°C. Positions derived from ARGOS are expected to be accurate to 111 m.

From February 1993, a total of 15 LCDs were deployed in Brazilian waters (Stevenson, 1996). First launched in the BC near 25°S, 44°W, five at a time in February 1993, July 1993 and January 1994, the LCDs were found in the BMC region from March 1993 to July 1994. As an unexpected result, out of the original set, three LCDs had drifted northwards from the BMC region penetrating the Brazilian Continental Shelf. These three LCDs were part of the first set of drifters launched at sea in February 1993.

The time series of latitude, longitude and temperature recorded by these three LCDs in the coastal current were processed to compute the main characteristics of this current during the time of the experiment. Table 1 shows the dates and geographical position of the beginning and end of the series used to describe the LCDs trajectories within the coastal current. The positional and temperature data series taken by the LCDs were

Table 1
LCDs time series in the BCC

Buoy	Date (Julian Day)		Latitude (°S)		Longitude (°W)	
	Start	Finish	Start	Finish	Start	Finish
3178	6 Apr. 1993 (96)	3 July 1993 (184)	28.59	23.10	48.02	44.37
3179	28 Apr. 1993 (118)	15 Oct. 1993 (288)	30.93	25.60	49.87	46.48
3180	21 May 1993 (141)	30 July 1993 (211)	33.30	24.59	50.79	45.02

also processed in terms of descriptive statistics and spectral analysis. For the spectral analysis the fast Fourier transform (FFT) method was used and the resulting spectra were smoothed by the utilisation of a Hamming windowing process (Press et al., 1992). The resulting energy peaks were all significant to the 95% confidence interval.

To estimate the current speed and direction, all the buoy positions were transformed from longitude and latitude into zonal and meridional displacements, respectively. Units were converted from the original degrees per day into cm/s. While the international recommendation is to use the International system (SI) units, the CGS units were used here in order to facilitate direct comparison with previously published results, essentially all of which are in CGS units.

Having the zonal and meridional displacements (x_i, y_i), and knowing the time interval (t) between two consecutive position measurements $(i, i+1)$, the zonal (u_i) and meridional (v_i) instantaneous velocities (cm/s) were computed as follows:

$$u_i = \frac{x_{i+1} - x_i}{t_{i+1} - t_i}, \quad v_i = \frac{y_{i+1} - y_i}{t_{i+1} - t_i}. \tag{1}$$

The mean zonal $(\bar{U})$ and meridional $(\bar{V})$ velocity components for each time series were given by

$$\bar{U} = \tfrac{1}{n-1}\sum_{i=1}^{n-1} u_i, \quad \bar{V} = \tfrac{1}{n-1}\sum_{i=1}^{n-1} v_i, \tag{2}$$

where n is the number of points in each positional time series.

The overall mean current velocity (V_m) and the mean current direction (θ_c) were obtained from

$$V_m = \sqrt{\bar{U}^2 + \bar{V}^2}, \quad \theta_c = \arctan(\bar{V}/\bar{U}), \tag{3}$$

where V_m is in cm/s and θ_c is in degrees. The final mean current direction, however, was transformed into the appropriate geographic bearing.

In order to examine the influence of time dependent, mesoscale perturbations present in each buoy trajectory, the positional time series were also used to compute the mean, eddy and total kinetic energies (*MKE*, *EKE* and *TKE*, respectively) as defined below. These energies were computed on a temporal basis, in contrast with some methodologies which use spatial averages (e.g. Schäfer and Krauss, 1995). This approach has the advantage of computing energies for each buoy time series, and is especially useful when one has a small number of tracks over a specific area or if the study area is not regularly covered by the tracks.

For the computation of the kinetic energies, it was assumed that the velocity of a fluid parcel, at a particular moment along its trajectory, was equal to the summation of the velocity of a mean current (V_m) and of a perturbation. The instantaneous zonal (u_i') and meridional (v_i') perturbation velocities were represented by the successive buoy detrended instantaneous velocities.

The mean kinetic energy (*MKE*) per unit mass was then computed from V_m by

$$MKE = \frac{{V_m}^2}{2}. \tag{4}$$

While V_m is given in cm/s, *MKE* is given in $\mathrm{cm}^2/\mathrm{s}^2$.

The eddy kinetic energy (*EKE*) is given by

$$EKE = \frac{U_{EKE} + V_{EKE}}{2}, \tag{5}$$

where U_{EKE} and V_{EKE} represent the time-averaged instantaneous zonal and meridional kinetic energy associated with the components of the detrended

velocities, given by

$$U_{EKE} = \frac{1}{n-1}\sum_{i=1}^{n-1} u_i'^2, \quad V_{EKE} = \frac{1}{n-1}\sum_{i=1}^{n-1} v_i'^2. \tag{6}$$

The total kinetic energy (*TKE*) was computed by adding the *MKE* and the *EKE* terms for each time series. All kinetic energies were estimated in CGS units (i.e. cm^2/s^2), since the currents were in cm/s units.

2.2. High-resolution images

High-resolution (1.1 km × 1.1 km at nadir) AVHRR images were obtained and recorded at the National Institute for Space Research (INPE, Brazil) for the COROAS project. Raw images were processed at the Southampton Oceanography Centre (SOC) to generate geolocated, 512 km × 512 km SST charts for the BMC region (26.4–42.7°S; 38.8–58.8°W). During the processing, original pixels within each column were resampled to a nominal 4 km × 4 km resolution. However, since the ingestion process reads one pixel and jumps three, each pixel within the ingested image still maintains the original 1.1 km × 1.1 km resolution.

SST maps were generated covering the period between 10 March 1993 and 11 July 1994 following the Multi-Channel Sea Surface Temperature (MCSST) algorithms provided by Kidwell (1995) for NOAA-11 and NOAA-12 satellites. Although INPE have recorded at least one full AVHRR scene per day during 1993 and 1994, high cloud coverage in the study area (especially in winter) has reduced the useful images to a total of 82.

The SST images obtained for the winter of 1993 and 1994 show strong thermal gradients between Brazilian Coastal Current (BCC) and BC, and the intrusion of BCC north of Santa Marta Cape is clearly revealed. As the primary objective of the geolocation made for the images was to have a multi-temporal set of images for the BMC region, the northern limit of them was set to be 26.4°S. A smaller set of processed images published elsewhere (e.g. Campos et al., 1996a, b) for the same period of this analysis has, however, indicated that the cold waters intrusion presented in our data set have penetrated north of 26.4°S. From the papers of Campos et al. (1996a, b), we can make a direct link between the northwards penetration of the coastal current as measured by the buoy trajectories and the position of the 20°C isotherm as estimated from the AVHRR data by the MCSST algorithms (Kidwell, 1995).

Papers dealing with the direct comparison between in situ and satellite SSTs in the region of the SWA are not very common in the literature. It is true that the general behaviour of the SST fields (main features, gradients, etc.) in the SWA can be assessed by MCSST-derived SST charts. However, accurate SSTs in satellite images can only be known by validating pixel SSTs with in situ SSTs. Souza (2000) has investigated the temperature differences between in situ and satellite SSTs with the data used here. The author compared coincident buoy, ships of opportunity and AVHRR SSTs in a time window of ±3 h. Souza (2000) has shown that the mean temperature difference between 'real' (in situ) buoy SSTs and AVHRR (MCSST-retrieved) SSTs was −1.5°C for the region and period of this study. In practice, this indicates that when we locate the 20°C isotherm in a satellite image of the SWA what in reality we are locating is the 18.5°C isotherm. This limit is pointed out by Campos et al. (1995) as the lower thermal limit of the TW in the SBB region.

2.3. Low-resolution images

The low-resolution images set used here consists of MCSST global data available from the JPL/NASA for the period between January 1982 and December 1995. Each image consisted of 2048 × 1024 pixels, from which a subset of 512 × 512 pixels was extracted to cover only the South Atlantic Ocean, from 20°N to 70°S, 20°E to 70°W. The pixel resolution is 18 km × 18 km. The images were also monthly averaged from daytime overpasses and fully interpolated to fill in gaps caused mainly by cloud cover in the original AVHRR images from where the MCSST is derived. This resulted in a total of 168 monthly mean sequential images for the South Atlantic Ocean.

MCSST algorithms are derived from a composite of different AVHRR infrared channels taken in pairs (split-window, dual-window) or all together (triple-window). The coefficients also depend on the time of the day (daytime, nighttime), satellite and on a statistical match with in situ data. That gives the MCSST a 'bulk-like' temperature response, with an accuracy of about 0.5°C (McClain et al., 1985). For more information about the MCSST algorithms and its evolution with time see Kidwell (1995).

At present, NASA is conducting a re-analysis of all its MCSST products in an attempt to homogenise SST estimates made in the past by different MCSST algorithms (the NOAA/NASA AVHRR Oceans Pathfinder project). At the time this work was performed, however, the availability of the Pathfinder data set was less than the 14 years long MCSST time series. Given its greater temporal coverage and to be consistent with other authors' results, the MCSST data set was chosen for use here rather than the Pathfinder data set.

Considering the water mass classification of the continental waters of Brazil and to be consistent with the findings of Campos et al. (1996a, b), we have assumed the MCSST-retrieved isotherm of 20°C as the lower thermal limit for TW all the year round. We assume that TW is only carried by BC flowing south-westwards, and the CW and/or SAW are carried north-eastwards inside the SBCS. The 20°C isotherm was located in each monthly averaged MCSST image as an indicator of the limit between TW and CW or SAW. The shape of this isotherm off the SBCS in all the 168 MCSST images was always a 'Z' shape, and the positions of its two extreme vertices were taken as the northernmost limit of the BCC and the southernmost limit of the BC.

The 'Z' shape of the 20°C isotherm through the year changed from being compressed during summer to being more stretched in winter. The positions of the BCC and BC extremes for each month from January 1982 to December 1995, as defined by the satellite data, were then treated as a time series. Because very high cloud coverage in the vicinity of 30°S resulted in extensive interpolation in the MCSST data set covering that area, the extreme positions of BCC and BC were not estimated for June 1988, June 1992, May–July 1993, April–September 1994 and March 1995.

In order to represent better the typical seasonal changes in the 20°C isotherm (which can also be interpreted as a proxy for the STF in the South Atlantic Ocean), another average was computed from the MCSST data for the same months in different years. For instance, the months of January 1982, January 1983 and so on until January 1995 were averaged to represent the 14 years long climatological average representing January. The same climatological average was performed for all other months and a climatological map of the STF monthly mean positions in the South Atlantic was then generated.

3. Results and discussion

3.1. Trajectories and high-resolution images

The trajectories described by the LCDs relative to 15 m depth waters at the BCC are seen in Fig. 2a. The trajectories had already been described in some of the previous COROAS papers (e.g. Campos et al., 1996a, b; Stevenson et al., 1998) although sometimes referred as 'the northbound flow of the BC recirculation scheme'.

Fig. 2a indicates that the BCC is flowing northeastwards parallel to the Brazilian coast on the SBCS in depths lower than 200 m. Eddy activity and meandering can also be noted along all trajectories. Major activity is seen at about 25°S, 46°W, in the region near the buoys' launching position. Souza (2000) describes the characteristics of the eddies found in the buoy trajectories and satellite images collected during the COROAS project. The author relates the features to their Rossby numbers and to the typical Rossby radius of deformation for the region and reports the typical sizes of the eddies found in the BMC and SBCS regions in 1993 and 1994.

Although the buoys were launched together at the BC in February 1993, they entered the BCC in different positions and at different times (Table 1) after April 1993. The time delay between the entrance of each single drifter in the BCC did not result in much difference between the trajectories

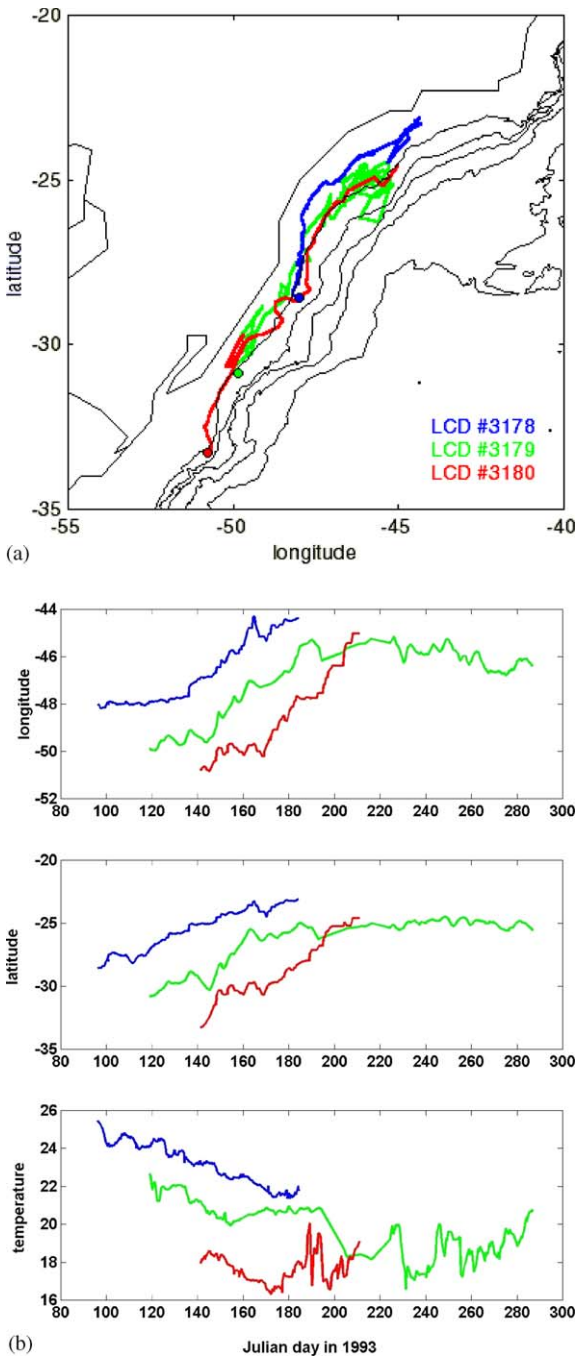

Fig. 2. (a) Trajectories described by the LCDs in the BCC. Individual buoy numbers are indicated. The beginning of each trajectory is marked with a circle. The bathymetry is consistent with Fig. 1. (b) Time series of longitude, latitude and temperature (°C) for the LCDs.

presented by the buoys. Due to cloud cover, it was very difficult to match precisely the entrance times of each buoy into the BCC from the BC with high-resolution AVHRR images. An image taken on 29 April 1993 (Fig. 3a), however, shows buoy 3179 entering the BCC from the BC, having been captured by a small-scale warm core eddy (~25 km wide) at the boundary between the BC and the BCC.

The overall set of AVHRR images show that the separation between the BC and the BCC is very distinct due to the strong thermal gradients between the waters transported by these currents. The winter images show also that the 20°C isotherm is located at the centre of the most prominent lateral thermal gradients between coastal and oceanic waters being, therefore, a good indicator of the geographical limits between these waters. Fig. 3 shows examples of the thermal gradients in question. Lateral mixing is suggested by the presence of shear instabilities caused by the two currents flowing in opposite directions. As noted in Fig. 3b, these instabilities occur all along the front line between the BC and the BCC, and suggest that the BC can feed the BCC at the surface by the detachment of warm core eddies. The BCC also ejects cold core rings into the BC.

Comparing the BCC/BC front thermal characteristics with the description of the Subtropical Shelf Front made by Piola et al. (2000), we can interpret that the former is only the surface signature of the last, being, therefore, restricted to the first 50 m depth water column. As shown in Piola et al.'s Fig. 7 (Fig. 4 in this paper), the nature of the Subtropical Shelf Front it that its surface signature extends farther north (about 2° in latitude) than the mean position of the rest of the front below the 50 m depth.

Figs. 3c and d present a 1-day sequence illustrating the development of a mushroom-like structure in the BC in the vicinity of Santa Marta Cape at 28°S. The process of surface interleaving between the BC and the BCC is clear from this figure, and two warm core, cyclonic rings about 50 km wide are in the process of formation in the BC to be expelled to the BCC. These instability features are probably not in geostrophic balance (since warm core rings are supposed to have an

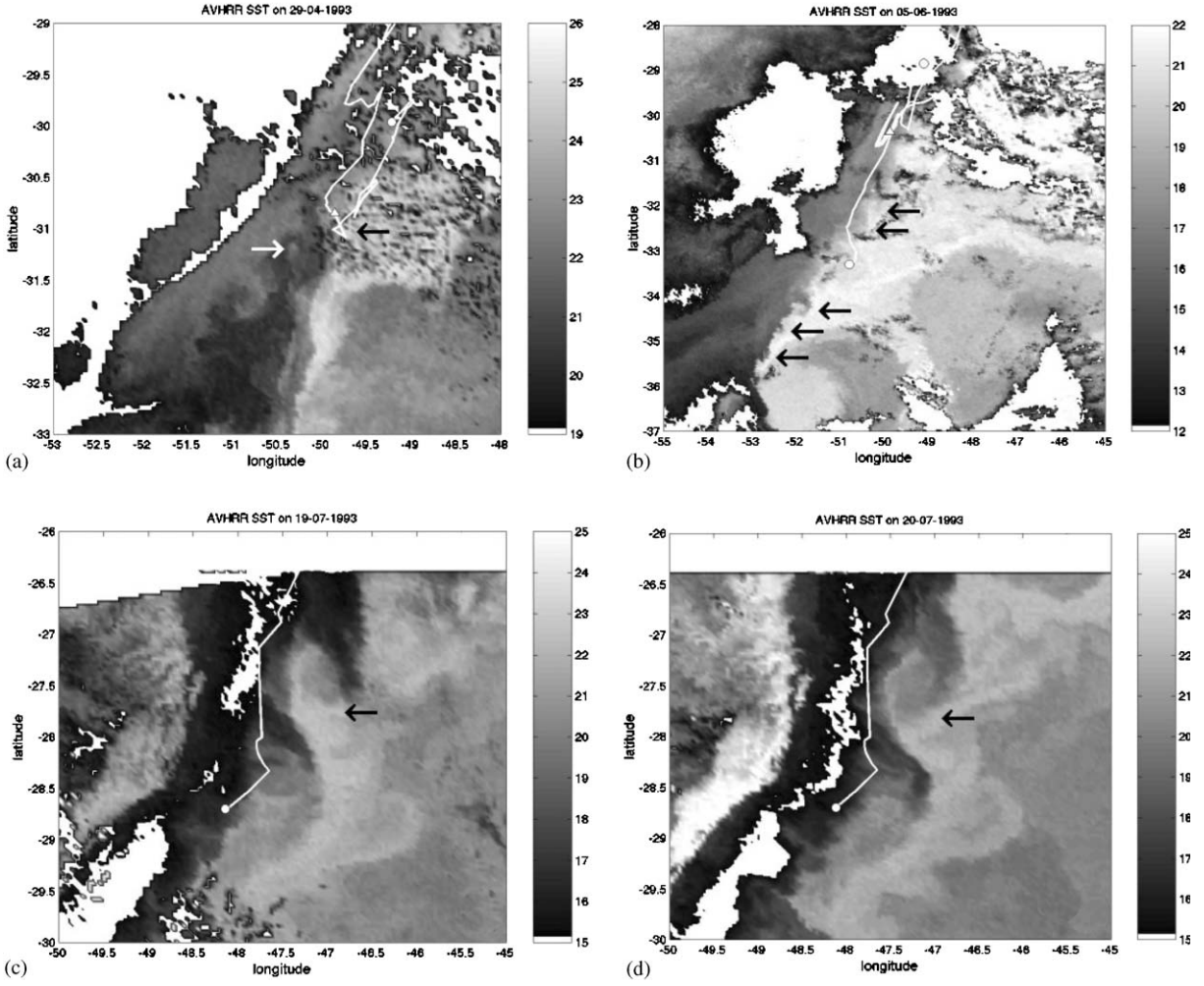

Fig. 3. (a) AVHRR image taken on 29 April 1993. The image shows buoy 3179 entering the BCC from the BC after having been captured by a small-scale warm core eddy visible in the buoy's track (indicated by the black arrow). The possible equivalent of this eddy in the AVHRR image is indicated by the white arrow. (b) The BC/BCC front at the SBCS in 5 June 1993. Buoys 3179 and 3180 tracks are seen in the image. Lateral mixing is suggested by the presence of shear instabilities caused by the two currents flowing in opposite directions. The arrows indicate the instability waves at the front. (c, d) One-day sequence of AVHRR images taken in 19 July 1993 (left) and 20 July 1993 (right) illustrating the development of a mushroom-like structure in the BC in the vicinity of Santa Marta Cape at 28°S (indicated by the arrows). Buoy 3180 track is seen in the 1-day sequence. In all images, the BCC is represented by the cold waters at the shelf, while the BC is represented by the warm waters offshore. The circles indicate buoy's position 20 days before the images' acquisition time, the triangle indicates the buoy position within ± 12 h from the image's acquisition time. The bar indicates the temperature in °C.

anticyclonic gyre in the Southern Hemisphere), but can probably account for much of the BCC/BC exchange of heat and momentum along the front.

Since lateral mixing and eddy formation happens along the full length of the BCC, it is supposed that the position at which a particular buoy launched in the BC penetrates the BCC through the front depends randomly on the location where this particular buoy is caught by a warm core eddy being formed. Both our Lagrangian

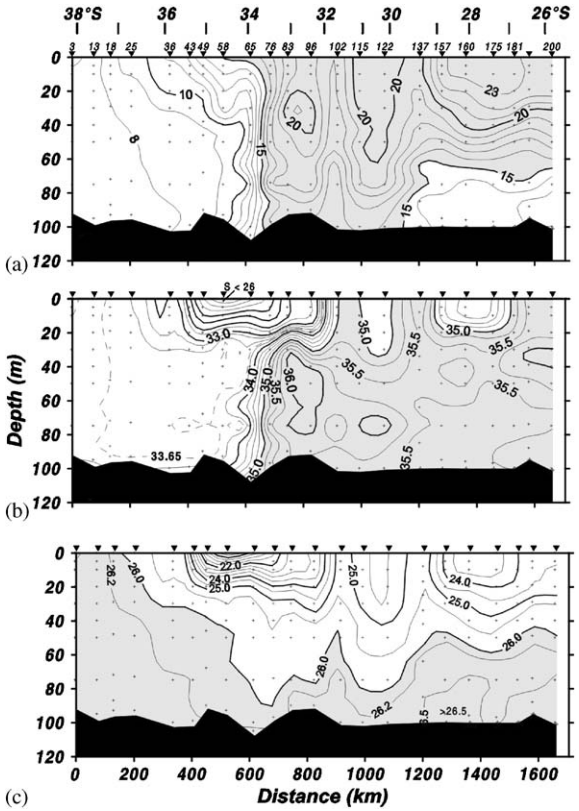

Fig. 4. Vertical sections of (a) temperature, (b) salinity and (c) density anomaly (σ_T) along the eastern South American shelf during the winter of 1977. The Subtropical Shelf Front is seen between the STSWs (grey) and the SASWs (white). *Source*: Piola et al. (2000).

and satellite observations have indicated that BC waters can enter the BCC all along the front between these two currents.

The observation of interleaving or instabilities along the BCC/BC front is also reported by Lima et al. (1996), who consider that the entrainment of cold core eddies originating in the CW at the shelf to the BC is an important mechanism for providing nutrients from coastal or Subantarctic origin to the oligotrophic TW. They also report that cold core eddies in the BC can induce upwelling at the shelf break and, together with the wind-driven circulation, produce a very distinct cross-shelf circulation regime from winter to summertime.

Early results from Lagrangian measurements made by the COROAS project in the SBCS suggested that the BC recirculates on the shelf (Stevenson and Souza, 1994; Stevenson, 1996). Following different paths along the SBCS, the period of recirculation computed from the LCDs' trajectories varied from 115 to 161 days. It was assumed that the BC return flow ends up becoming part of the MC extension inside the SBCS between 33°S and 23°S, although no explanation was proposed. Our data suggest that in fact the BC does not recirculate inside the SBCS but exchanges mass and heat with the BCC through turbulence along its western limit.

According to Loder et al. (1998), the majority of the ocean's western boundary currents flow along the outer shelf or continental slope, providing a large source of momentum and water mass properties to the coastal region due to their substantial associated volume transport. Loder et al. (1998) add that one of the best known forms of eddy activity affecting the western boundary shelves is the transient warm core eddy generation from meanders of subtropical western boundary currents. Other effects such as entrainment, vorticity waves, and on-shelf intrusions or buffering water masses are quoted as also producing major influences from boundary currents in the adjacent continental shelves and CW. The western boundary currents' influence on CW, however, decreases with increasing shelf width. In the SBCS, for instance, the BC wintertime influence on the shelf can be expected to be greater in the region of Santa Marta Cape, where the shelf is only about 70 km wide.

The time series of latitude, longitude and temperature measured by the LCDs are seen in Fig. 2b. Although entering the BCC on different dates, all time series show similarities in their initial measurements when the buoys were flowing north-eastwards. Each temperature time series contains a quasi-constant cooling rate of about 0.12°C/day when the buoys were travelling north-eastwardly in the BCC. Temperature measurements made by buoy 3179, for example, decay from about 22°C to 20°C during the part of the trajectory when the buoy was flowing north-eastwards.

Lentini et al. (2001) have studied the annual cycle of the SST in the SWA. By using a similar

data set as the MCSST data set used here, the authors have presented the time series of SST from 1982 to 1994 at eight selected points on the continental shelf from 38°20′S to 24°23′S. The seasonal cooling rates which can be inferred from Lentini et al. (2001) paper for the shelf are between 0.03°C/day and 0.07°C/day. Higher cooling rates occurr at the La Plata River mouth and to the south of it. Most of the points in the SBCS present cooling rates of about 0.04°C/day, which is three times smaller than the rate presented by our drifting buoy measurements in the BCC.

The SST measurements made by buoy 3179 are consistent with the SST image presented in Fig. 3a. The small-scale warm core eddy shown in Fig. 3a presents a temperature of about 22°C and is surrounded by BCC waters at about 20°C. This evidence, together with the knowledge that the cooling rate presented by the SSTs measured by the buoys are about three times bigger than expected for the shelf waters, leads to an interpretation that the LCDs entered the cooler BCC surrounded by warmer BC waters. The mechanism responsible for that is probably the shedding of small-scale eddies. Due to mixing, and consistent with the eddy dissipation, the temperatures measured in the initial part of the LCDs trajectories decay with time.

3.2. Current velocity, kinetic energies and temperatures

The mean current speed and direction, kinetic energies and basic statistics for the time series derived from the LCDs are seen in Table 2. Average surface (15 m depth) speed found for the BCC was 11 cm/s (std. dev. = 6 cm/s) and the mean direction was 27° (std. dev. = 11°). From the trajectories, one can see that the BCC can reach the vicinity of 23°S. The mean speed found here for the BCC is high in comparison to the value of 1.8 cm/s found by Zavialov et al. (2002) for the along-shelf coastal current at the 15 m depth. If only the first 32 days of the current meters time series is taken into consideration (when both 15 and 40 m depth current meters were functioning together), however, Zavialov et al. (2002) found mean along-shore currents of 16 cm/s (15 m) and 8 cm/s (40 m) with data correlated with a coefficient of about 0.9. It is worth remembering, however, that although both buoy and current meter data can be compared, drifting buoys are Lagrangian instruments, measuring changing currents both in space and time while current meters are Eulerian instruments in this case fixed to a location at the shelf close to 32°S.

From the buoy data presented here we can say that the BCC, in comparison to the BC, is relatively slow and flows in the opposite direction to the latter. The BC velocity estimates and measurements, although still sparse, are much more frequent than those in the BCC. Lagrangian estimates made by Stevenson and Souza (1994), Stevenson (1996), Souza and Robinson (1998) and Souza (2000) using the COROAS data set have demonstrated that the BC speed varies from 15 to about 50 cm/s and that the current flows southwestwards. They agree with Schäfer and Krauss (1995) that the BC velocities tend to increase as the current goes south towards the BMC region. The

Table 2
BCC velocity, kinetic energy and temperature statistics

Buoy	Velocity		Kinetic energy				Temperature	
	Speed (cm/s)	Direction (degrees)	*MKE* (cm^2/s^2)	*EKE* (cm^2/s^2)	*TKE* (cm^2/s^2)	% *EKE*/*TKE*	Average (°C)	Std. dev. (°C)
3178	10	35	50	2384	2434	97.9	23.34	1.08
3179	6	15	17	771	788	97.8	19.82	1.43
3180	17	31	145	2089	2234	93.5	17.63	0.82
Average	11	27	71	1748	1819	96.4	20.26	1.11
Std. dev.	6	11	66	859	898	2.5	2.88	0.31

latter deployed more than 130 satellite-tracked drifting buoys in the South Atlantic between 1990 and 1993. They measured the major currents in the SWA and in the Antarctic Circumpolar Current (ACC). Although they do not calculate any statistics for the BCC, the authors indicate the tracking of a BC coastal counter current by two of their buoys.

Based upon previous measurements by three other authors and predictions by a model, Castro and Miranda (1998) have also indicated that seasonal currents flow predominantly along the SBB shelf towards the north-east. They pointed out that measurements of currents in the inner SBB are very few, but indicated that north-easterly currents are more frequent and more intense (30–40 cm/s) during wintertime, owing to the presence of south-westerly winds.

Table 2 indicates that the *MKE* in the BCC varied from 17 to 145 cm^2/s^2, while the *EKE* varied from 771 to 2384 cm^2/s^2. Souza and Robinson (1998), together with estimates for the BCC made with one of the buoys used here, have presented *MKE* and *EKE* estimates for the BC and for the South Atlantic Current (SAC). In the mean, the BC *MKE* was 801 cm^2/s^2 and the SAC *MKE* was 59 cm^2/s^2. Mean *EKE* estimates for the BC and the SAC were 1294 and 3268 cm^2/s^2. That represents, respectively, 61.7% and 98.4% of the *TKE* present in the currents. The result shown here for the BCC indicates that this current, as well as the SAC, concentrates more than 95% of its energy in small-scale perturbations and eddy activity rather than in the mean flow. Schäfer and Krauss (1995) have estimated that the MC *EKE* is about 500 cm^2/s^2, but a maximum of 1600 cm^2/s^2 in the BMC region was found, decreasing again farther east in the SAC. This indicates that the BCC and the SAC, both extensions of the BC and the MC, respectively, seem to be less stable and more energetic than their principal originators.

Table 2 also contains the temperature statistics for the BCC. A mean value of 20.26°C was found for this current. This mean is higher than that expected for the BCC from the satellite measurements, where the tongue of cold waters has typical SSTs of 15–17°C and can only be explained by the presence of warm water from the BC being advected in the BCC. As discussed before, the buoys were probably being carried by dissipating warm core eddies inside the BCC and, therefore, the temperature measurements made by them can probably not be truly representing the BCC overall.

3.3. BCC time series FFT spectra

The FFT analysis of the buoys' time series in the BCC revealed the presence of energy peaks significant at the 95% confidence level at periods varying from 103.1 to 1.5 days (Fig. 5 and Table 3). A peak at 103.1 days was found in the temperature and instantaneous meridional velocity time series of buoy 3179. A peak at 70.4 days was present in the instantaneous meridional velocity series of buoy 3179. Both the time series of temperature of buoy 3178 and the instantaneous meridional velocity of buoy 3180 presented a peak at 51.3 days. Towards the lower periods, high energy peaks were most commonly found at about 34–35, 29–30, 20–23, 10–13 and 6–7 days. Many other peaks are distributed at lower periods down to about 2 days. The energy peaks found for the BCC are generally distinct from those found for the BC and the SAC, which were described by Souza (2000) for the same period of this analysis. An exception to that occurs at the periods close to 10–13 days which are mainly present in most of the BC time series but also in some of the SAC and BCC series.

According to Castro and Miranda (1998), the current variability in the middle and inner SBB shelf is dominated by subtidal and tidal oscillations. Large energy peaks, however, are concentrated in the periods of 3–7 and 9–15 days, the same as the wind and sea level oscillations. These authors, for instance, reported that the occurrence of the frontal systems (which are driving the winds' intensity and direction) over the SWA between 20°S and 34°S has a time scale of 5–10 days between passages.

Working with wind data in the SBB, Stech and Lorenzzetti (1992) found peaks of 11 and 6.5 days for their frequency spectra. By analysing sea level data in the same region, they demonstrate the existence of a peak centred at 7 days, which was

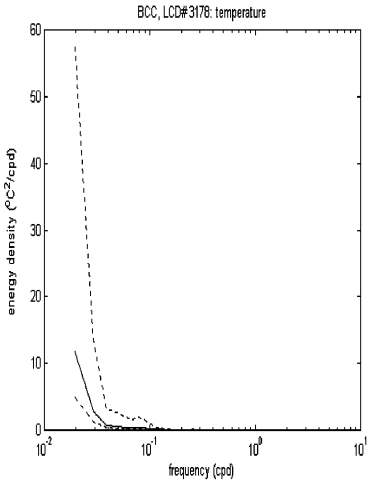
BCC, LCD#3178: temperature
energy density (°C²/cpd)
frequency (cpd)

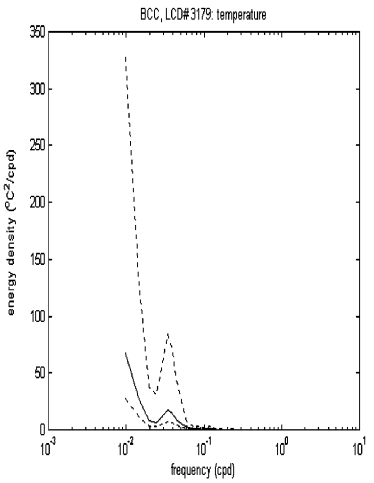
BCC, LCD#3179: temperature
energy density (°C²/cpd)
frequency (cpd)

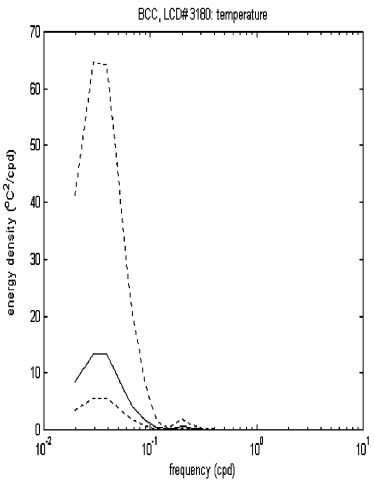
BCC, LCD#3180: temperature
energy density (°C²/cpd)
frequency (cpd)

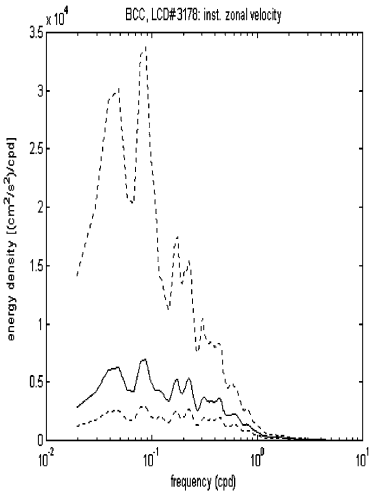
BCC, LCD#3178: inst. zonal velocity
energy density [(cm²/s²)/cpd]
frequency (cpd)

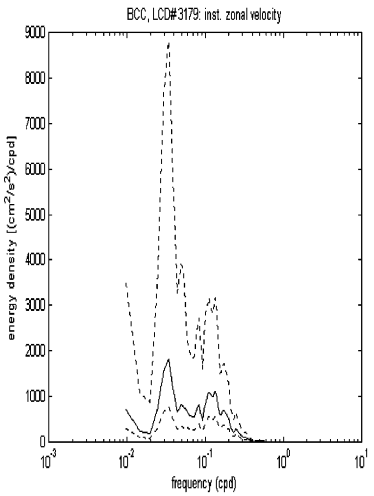
BCC, LCD#3179: inst. zonal velocity
energy density [(cm²/s²)/cpd]
frequency (cpd)

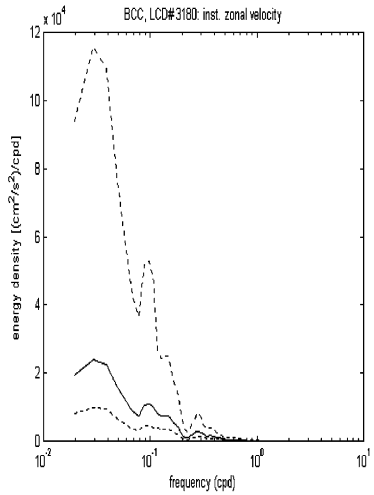
BCC, LCD#3180: inst. zonal velocity
energy density [(cm²/s²)/cpd]
frequency (cpd)

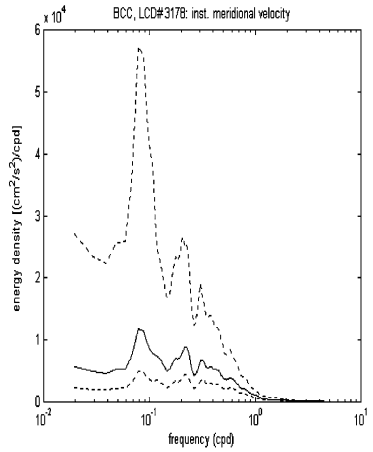
BCC, LCD#3178: inst. meridional velocity
energy density [(cm²/s²)/cpd]
frequency (cpd)

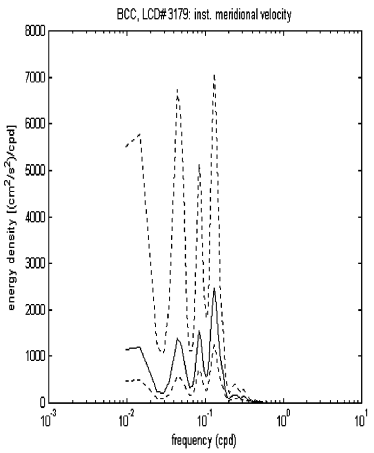
BCC, LCD#3179: inst. meridional velocity
energy density [(cm²/s²)/cpd]
frequency (cpd)

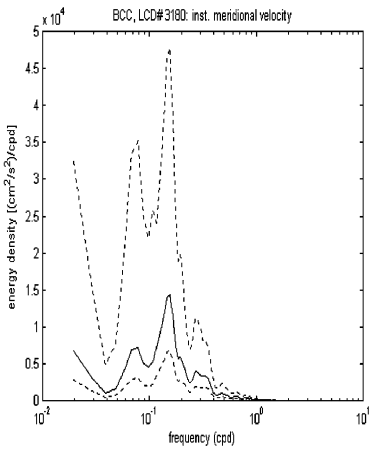
BCC, LCD#3180: inst. meridional velocity
energy density [(cm²/s²)/cpd]
frequency (cpd)

Table 3
Period of the major energy peaks for the buoys' temperature and instantaneous velocity time series in the BCC (dominant periods underlined)

Buoy	Temperature (days)	Zonal instantaneous velocity (days)	Meridional instantaneous velocity (days)
3178	51.3	20.7; 11.5; 5.8; 4.5; 3.3; 2.3; 1.7	12.6; 5.7; 4.6; 3.3; 1.7
3179	103.1; 28.9	103.1; 29.5; 20.2; 12.1; 9.2; 7.4; 5.9; 4.0	70.4; 23.1; 12.1; 7.8; 4.2; 3.2
3180	34.5; 5.0	33.9; 10.4; 6.9; 3.6; 2.7	51.3; 13.0; 6.5; 3.6; 3.0; 2.1; 1.5

associated with the atmospheric pressure systems crossing the SBB. They pointed out that the passage of low-pressure atmospheric systems is one of the major forcing mechanisms present in the SBB during wintertime. The cold atmospheric fronts occurring in the SBB were reported to have a displacement speed of 500 km/day in the south-west to north-east direction. This is the same direction as the BCC current.

Stevenson et al. (1998), studying the intrusion of cool waters in the SBCS, also considered that atmospheric forcing would drive the north-easterly currents in that region, and can be the principal reason for the intrusion of cool waters of Subantarctic origin to about 22°S in the SBCS. Similar results were found by Zavialov et al. (2002) when presenting the frequency spectra of their current meter data at the continental shelf of southern Brazil. The authors reported that, in both across-shore and along-shore components of the coastal currents, more than 50% of the kinetic energy is related to the meteorological forcing in periods between 2 and 10 days.

Johannenssen et al. in 1967 and Mesquita and Leite in 1986, both cited by Castro and Miranda (1998), estimated that an annual wave dominates sea level variability in the SBB. High values occur during autumn and winter. Current variability in the middle and inner SBB shelf, according to Castro and Miranda (1998), is dominated by subtidal and tidal oscillations. Large energy peaks are concentrated at 3–7 and 9–15 days, the same as the wind and sea level oscillations.

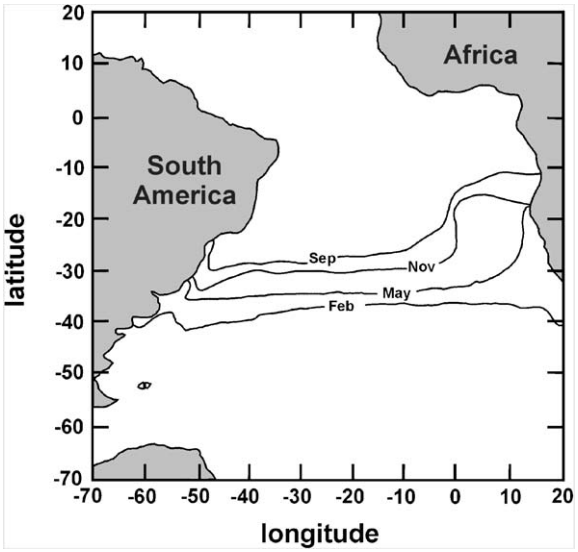

Fig. 6. Oscillation of the STF as seen by the 20°C isotherm displacement taken from the monthly averaged climatological MCSST images. The southernmost line represents the month of February while the northernmost line refers to September. May, November and the other consecutive months (not shown) are displaced between February and September.

3.4. Subtropical Front seasonal oscillation

Fig. 6 shows the mean seasonal oscillation of the STF produced from MCSST monthly climatological averages between 1982 and 1995. The oscillation of the STF is represented by the monthly displacement of the 20°C isotherm. In the open South Atlantic Ocean, the north and

Fig. 5. Energy preserving spectra of the LCD nos. 3178 (left column), 3179 (middle column) and 3180s (right column) temperature (upper panels), zonal instantaneous velocity (middle panels) and meridional instantaneous velocity (lower panels) time series in the BCC. The dashed lines represent the 95% confidence interval.

south extremes for the STF occurred during September and February, respectively. In the open ocean, the isotherms tend to have a quasi-zonal orientation. From about 5°E and 48°W towards the African and American continents, respectively, however, the isotherms are bent by the boundary currents.

The migration distance of the SFT through the year is about 1000–1200 km in the open ocean, while in the boundary to the African continent this range is greater than 2000 km. In the BMC and SBCS regions, the 20°C isotherms take the 'Z' form previously mentioned, migrating about 1600 km from winter to summertime. From Fig. 6, we can suppose that the penetration of the BCC in the SBCS in wintertime has a direct relation with the displacement of the STF towards the north in this season of the year. Although no statistical analyses have been performed to correlate the STF oscillation with the direct measurements in the BCC during COROAS, we suggest that the front seasonal oscillation is of great importance for driving the penetration of the BCC inside the Brazilian shelf.

Considering that the BMC region is the western extreme of STF, it is known that the confluence oscillation is directly linked with the seasonal oscillation of the STF. In the same way, the Subtropical Shelf Front (of which the BCC/BC front is considered in this paper the surface signature) is considered by Piola et al. (2000) as an extension of the BMC over the continental shelf, being influenced by the seasonal changes of the BMC location as well as the STF location.

Nevertheless, Peterson and Stramma (1991) pointed out that the reasons for the BMC oscillation are still not clear. Possible causes include interaction with the large-scale atmospheric seasonal cycles in the central South Atlantic. For instance, the subtropical atmospheric pressure system in this ocean moves its centre of high pressure northwards in the winter, intensifying at the same time. Besides, the South Equatorial Current (SEC), which feeds the BC, is also strengthened and displaced to the north in the wintertime, and the zero-line of the wind stress curl is shifted 5° in latitude north from its mean position in the summer. Garzoli and Garraffo (1989) also attributed the spatial variation of the BMC to the variability of the winds and of the SEC.

According to Olson et al. (1988), the local wind stress curl may also play a role in the location where the BC separates from the coast, forming

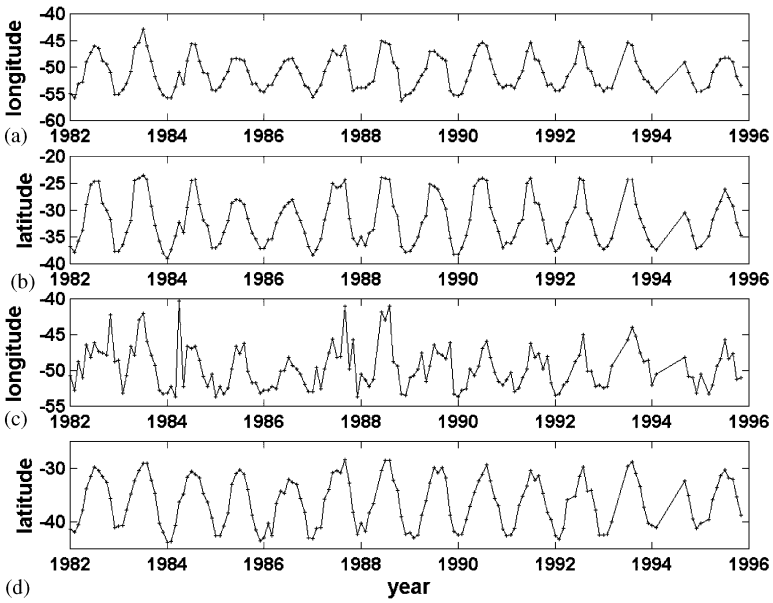

Fig. 7. Extreme position time series for the (a) BCC longitude, (b) BCC latitude, (c) BC longitude and (d) BC latitude.

the SAC and indicating the BMC southernmost limit. The variation in the MC forced by variations in the ACC system also plays a role in the process. Pressure changes in the Subantarctic Front, where the MC is fed by a branch of the ACC, could reach the BMC region by topographic Kelvin waves. Wind induced advective changes in the MC can also link the Antarctic sector with the BMC region.

3.5. BCC and BC extreme positions

Fig. 7 shows the extreme position time series for both the BCC and BC taken from the MCSST images between January 1982 and December 1995. Peaks in the time series are associated with the wintertime. The annual cycle and the seasonal oscillation of the BCC and BC extremes are clear. Since the oscillation of the BCC is parallel to the Brazilian coast, westwards displacement is coupled with southwards movement, and eastwards movement has its northwards counterpart. The BC longitude extremes time series (Fig. 7c) is noisier than the others, and the zonal displacement of this current is wider, as expected. BC southernmost extremes are located in the origin of the SAC, and its position is not restricted to the continental shelf.

The most southerly and northerly extremes found for the BCC were 39.1°S and 23.6°S occurring in February 1984 and August 1983, respectively. The difference between these extreme positions for the BCC is about 1700 km. Campos et al. (1999) report that cold SST anomalies dominated the SBCS at a 100 m along-shelf transect during 1982 and 1983. The most northerly latitudinal penetration of the BCC coincides in time with the cold anomalies described by Campos et al. (1999). These authors also made a direct link between these anomalies and the dramatic El Niño event of the same period.

For the BC, the most southerly and northerly latitudinal extremes were 43.8°S and 28.3°S in February 1984 and October 1987, respectively. The occurrence of both extremes can also have a link to El Niño events in the Pacific. Lentini et al. (2001) investigated further the SST anomalies in the SWA in the period between 1982 and 1994. The authors observed the presence and propagation of 13 cold and seven warm SST anomalies over the South American shelf and reported a relation between them and the El Niño–Southern Oscillation (ENSO). In their analyses, however, the seasonal components of the SST measurements were removed to provide a better understanding of the interannual fluctuations in the study region.

Table 4 and Fig. 8 show the basic statistics (mean and standard deviation) resulting from the BCC and BC extreme position locations for each month from January 1982 to December 1995. August was the month when the mean BCC and BC reached their northernmost limits. The mean

Table 4
Statistics for the BCC and BC extreme positions along the year

Month	Latitude BCC (°S)		Longitude BCC (°W)		Latitude BC (°S)		Longitude BC (°W)	
	Mean	Std. dev.	Mean	Std. dev.	Mean	Std. dev.	Mean	Std. dev.
Jan.	36.8	0.9	54.1	0.8	41.3	1.4	52.1	1.7
Feb.	37.2	1.0	54.7	0.7	42.0	1.1	51.9	1.5
Mar.	36.8	0.6	54.3	0.8	42.0	1.0	51.8	1.2
Apr.	34.1	0.5	53.3	0.5	40.4	1.4	51.0	1.6
May	32.4	0.6	51.4	0.7	36.7	1.1	49.8	3.5
Jun.	29.4	2.8	49.4	1.8	34.2	1.1	49.7	1.9
July	26.5	2.3	47.4	1.4	32.1	1.6	47.3	2.7
Aug.	25.2	1.6	46.3	1.6	30.3	1.0	46.2	1.9
Sep.	25.8	1.8	47.0	1.2	30.5	1.3	46.4	2.2
Oct.	29.1	1.7	48.9	1.0	31.9	1.5	47.7	2.3
Nov.	31.8	1.1	50.9	1.0	34.5	1.7	49.8	1.2
Dec.	34.6	1.3	53.3	1.3	38.3	1.5	49.9	3.3

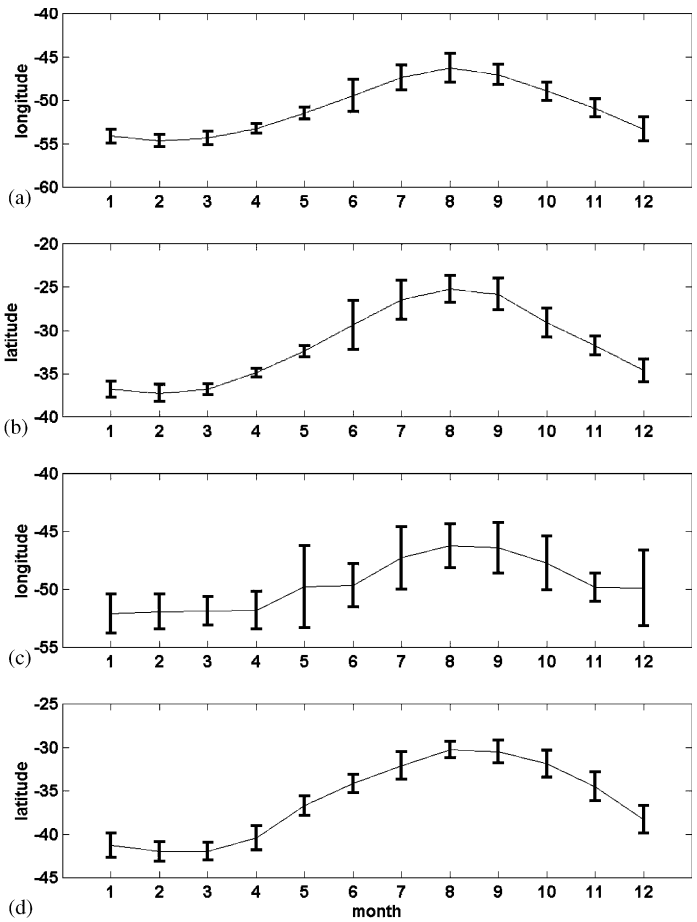

Fig. 8. Statistics per month of the extreme positions: (a) BCC longitude, (b) BCC latitude, (c) BC longitude and (d) BC latitude.

north extreme for the BCC was 25.2°S (std. dev. = 1.6°), and for the BC was 30.3°S (std. dev. = 1°). For the southernmost extremes, the mean latitude presented by the BCC was 37.2°S (std. dev. = 1°), and by the BC was 42°S (std. dev. = 1°). Hence, the BCC was found to oscillate an average 12° in latitude, which represents ~1330 km. The BC, on the other hand, was found to oscillate an average of about 11.7° in latitude or ~1300 km.

Reid et al. (1977) report that the position at which the BC reverses its direction (BC southernmost extreme) is between 40°S and 46°S. These authors add that this position is further south of the mean BMC oscillation region. Legeckis and Gordon (1982) found the latitudes of 38°S to 46°S as the maximum limits for warm water related to the BC. The southernmost extreme of BC occurrence found in this work (42°S ± 1° std. dev.) is in agreement to those found by Reid et al. (1977) and Legeckis and Gordon (1982). As it was not their objective, neither paper accounts for the northernmost extreme of MC (or BCC) along the South American coast.

Working with AVHRR data collected between July 1984 and June 1987, Olson et al. (1988) established the statistical characteristics of the separation region from the continental shelf (position of crossing with the 1000 m isobath) for both the BC and MC. Considering the BC, these authors found that this current separates from the coast at the mean latitude of 35.8°S, with a standard deviation of 1.1°. However, the total

range of latitudes where BC separates from the coast (difference between maximum and minimum values) was found to be 4.8°. This value is less than half the value of 11.7° found here for the BC oscillation. Causes for this disagreement are possibly related to the different methodologies employed to describe the BC extremes by Olson et al. (1988) and in this paper. While Olson et al. (1988) described the position where BC separated from the coast at the 1000 m isobath, here we have located the position where the 20°C isotherm reached its southernmost extreme in the BMC region. Besides this, the time series used here is far more extensive than the one used by Olson et al. (1988), which was restricted to 1984–1987.

As noted in Fig. 7b, the years of 1985 and 1986 (both included in Olson's paper) are also seen in the time series as years when the BCC had its wintertime northernmost limits reduced by about 3° in latitude with respect to adjacent years. This leads to an interpretation that 1985 and 1986 have had anomalously mild winters, which reduced the penetration of the BCC. Explanations for that cannot rely on the occurrence of El Niño, for instance, since this phenomenon occurred neither in 1985–1986 nor in 1994. In the winters of 1985–86, the La Plata River also did not present any anomalous outflow in relation to adjacent years (R.A. Guerrero, pers. comm.). That rules out the possibility of extra freshwater inflow being provided to the BCC waters.

Fig. 9 displays the BCC and BC extreme positions along the South American coast for the different seasons of the year (summer: Dec.–Feb.; autumn (fall): Mar.–May; winter: June–Aug.; spring: Sep.-Nov.). It seems that the vicinity of 32°S marks the extremity of occurrence of the BCC during summer and autumn months. The BCC only penetrates the SBCS north of 32°S during the winter or spring months. The neighbourhood of 32°S is reported by Lentini et al. (2001) as a nodal point (area of zero residual variance) for the spatial amplitudes of the SST residuals Principal Components mode 2 (21.7% of the total variance). Following Lentini et al. (2001), the 32°S latitude divides the SWA into two distinct regions marked by large negative (La Plata River region) or positive (SBB region) eigenvectors.

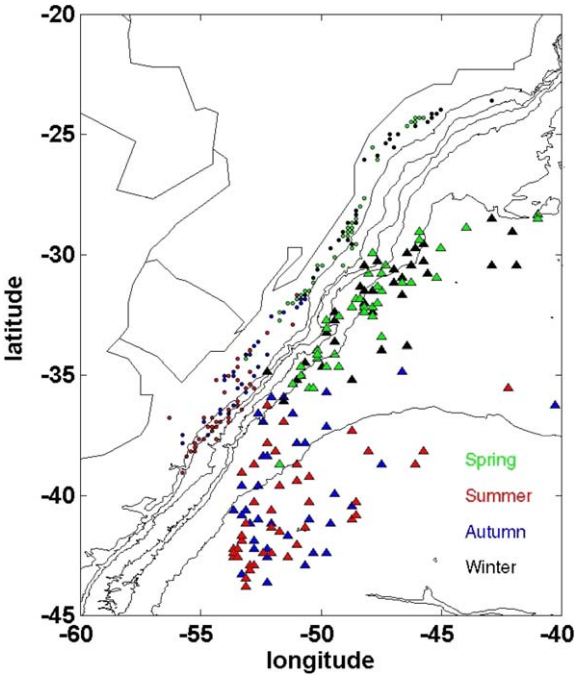

Fig. 9. BCC (circles) and BC (triangles) extreme positions per season in the SBCS. The bathymetry is consistent with Fig. 1.

The BCC extreme positions, as seen by the distribution of the small circles in Fig. 9, are continuous along the SBCS and restricted to isobaths shallower than 200 m in the inner shelf. This distribution is the same presented by the LCDs' trajectories in 1993 (Fig. 2a). The BC distribution for all seasons, on the other hand, is broader and not shelf-constrained.

4. Final remarks

The BCC is described as a relatively slow but highly energetic coastal current, flowing in the opposite direction to the BC. The current occurs over the SBCS during spring to wintertime, reaching its most northerly extreme at the mean value of 25.2°S in August every year.

High-resolution satellite imagery and WOCE standard LCDs used in conjunction demonstrated

that warm core rings expelled from the BC enter the BCC and can be advected north-eastwardly within the later. MCSST data demonstrated that the penetration of BCC on the SBCS to latitudes of about 25°S is probably not anomalous but rather the normal process happening most years on the Brazilian Continental Shelf. One of the principal mechanisms to drive the BCC penetration is believed to be more related to the large-scale oscillation of the STF in the open South Atlantic Ocean than with the local winds at the Brazilian coast.

Remaining questions to be answered about the BCC behaviour concern its relation with the discharge cycles in the La Plata River and Patos Lagoon, the local winds along the Brazilian shelf and the oscillation of the STF. Although the STF oscillation in the South Atlantic Ocean is supposed here to be one of the major forces governing the BCC intrusion further north on the Brazilian shelf, the local winds blowing from the south have a contribution which needs to be better understood. Ekman transport and sea level elevation (which depends on the continental outflow among other factors) are indicated by Zavialov et al. (1998) to be the forcing mechanisms for the northbound currents occurring at the southern part of the SBCS.

A better understanding of the BCC requires further direct measurements of this current in the SBCS. If the latitude of 32°S is actually a limit where the BCC occurs only in spring and wintertime, current meter or CTD moorings and LCD deployments should be carried out north of this latitude to confirm the seasonal character of this current. The use of sequential high-resolution AVHRR images to locate and track warm core eddies being expelled from the BC in the BCC should increase our understanding of the rates of formation of these structures at the BCC/BC front, and give us a better insight on their dissipation process. TOPEX/POSEIDON data could also be used to correlate seasonal variations of the sea surface height (SSH) with the presence of the BCC in the SBCS. In this case, however, a specific tidal model for the SBCS region should be developed and applied in order to obtain accurate SSHs over the area.

Acknowledgements

The authors wish to thank Merritt Stevenson and João Lorenzzetti (INPE), WOCE Global Data and JPL/NASA for providing the data. Paulo Sumida, Paolo Cipollini and Carlos Lentini are acknowledged for their encouragement and discussions. Osmar Möller, Edmo Campos and the anonymous reviewers provided very useful comments to the final text. The first author was funded by CNPq (201146-95.9). Funds for COROAS project were provided by CNPq, FAPESP and CIRM.

References

Campos, E.J.D., Gonçalves, J.E., Ikeda, Y., 1995. Water mass characteristics and geostrophic circulation in the South Brazil Bight: summer 1991. Journal of Geophysical Research 100 (C9), 18537–18550.

Campos, E.J.D., Lorenzzetti, J.A., Stevenson, M.R., Stech, J.L., Souza, R.B., 1996a. Penetration of waters from the Brazil–Malvinas Confluence region along the South American Continental Shelf up to 23°S. Anais da Academia Brasileira de Ciências 68 (Suppl. 1), 49–58.

Campos, E.J.D., Ikeda, Y., Castro, B.M., Gaeta, S.A., Lorenzzetti, J.A., Stevenson, M., 1996b. Experiment studies circulation in the Western South Atlantic. EOS, Transactions of the American Geophysical Union 77(27), 253, 259.

Campos, E.J.D., Lentini, C.D., Miller, J.L., Piola, A.R., 1999. Interannual variability of the sea surface temperature in the South Brazil Bight. Geophysical Research Letters 26 (14), 2061–2064.

Castro, B.M., Miranda, L.B., 1998. Physical oceanography of the Western Atlantic continental shelf located between 4°N and 34°S, coastal segment (4,W). In: Robinson, A.R., Brink, K.H. (Eds.), The Sea, Vol. 11. Wiley, New York.

Ciotti, A.M., Odebrecht, C., Fillmann, G., Möller Jr., O.O., 1995. Freshwater outflow and subtropical convergence influence on phytoplankton biomass on the Southern Brazilian Continental Shelf. Continental Shelf Research 15 (14), 1737–1756.

Defant, A., 1936. Die troposphäre. Deutsche Atlantische Expedition "Meteor" 1925–1927. Wiss. rg., Bd. VI, Teil I, 3. Lief., 289–411.

Emílsson, I., 1959. Alguns aspectos físicos e químicos das águas marinhas brasileiras. Ciencia e Cultura (Sao Paulo) 11 (2), 44–54.

Emílsson, I., 1961. The shelf and coastal waters off southern Brazil. Boletim do Instituto Oceanografico (Sao Paulo) 11 (2), 101–112.

Garcia, C.A.E., 1997. Physical oceanography. In: Seeliger, U., Odebrecht, C., Castello, J.P. (Eds.), Subtropical

Convergence Environments: the Coast and Sea in the Southwestern Atlantic. Springer, Berlin, Heidelberg.

Garfield III, N., 1990. The Brazil Current at subtropical latitudes. Ph.D. Thesis, University of Rhode Island, USA, 122pp.

Garzoli, S., Garraffo, Z., 1989. Transports, frontal motions and eddies at the Brazil–Malvinas Currents Confluence. Deep-Sea Research 36 (5), 681–703.

Guerrero, R.A., Piola, A.R., 1997. Masas de agua en la plataforma continental. In: Boschi, E.E. (Ed.), El mar argentino y sus recursos pesqueros, Tomo 1, Antecendentes históricos de las exploraciones en el mar y las características ambientales. INIDEP, Secretaría de Agricultura, Ganadería, Pesca y Alimentación, Mar del Plata, Argentina.

Guerrero, R.A., Acha, E.M., Framiñan, M.B., Lasta, C.A., 1997. Physical oceanography of the Río de la Plata Estuary, Argentina. Continental Shelf Research 17 (7), 727–742.

Kidwell, K.B., 1995. NOAA Polar Orbiter Data users guide (TIROS-N, NOAA-6, NOAA-7, NOAA-8, NOAA-9, NOAA-10, NOAA-11, NOAA-12, NOAA-13 and NOAA-14). NOAA/NESDIS National Climatic Data Center, Satellite Data Services Division, Washington, DC.

Legeckis, R., Gordon, A.L., 1982. Satellite observations of the Brazil and Falkland Currents —1975 to 1976 and 1978. Deep-Sea Research 29, 375–401.

Lentini, C.A.D., Podestá, G.G., Campos, E.J.D., Olson, D.B., 2001. Sea surface temperature anomalies on the Western South Atlantic from 1982 to 1994. Continental Shelf Research 21, 89–112.

Lima, I.D., Garcia, C.A.E., Möller Jr., O.O., 1996. Ocean surface processes on the Southern Brazilian Shelf: characterization and seasonal variability. Continental Shelf Research 16 (10), 1307–1317.

Loder, J.W., Boicourt, W.C., Simpson, J.H., 1998. Western ocean boundary shelves coastal segment (W). In: Robinson, A.R., Brink, K.H. (Eds.), The Sea, Vol. 11. Wiley, New York.

Longhurst, A., 1998. Ecological Geography of the Sea. Academic Press, San Diego, 398pp.

McClain, E.P., Pichel, W.G., Walton, C.C., 1985. Comparative performance of AVHRR-based multichannel sea surface temperatures. Journal of Geophysical Research 90, 11587–11601.

Miranda, L.B., 1972. Propriedades e variáveis físicas das águas da plataforma continental do Rio Grande do Sul. Ph.D. Thesis, Instituto de Física, USP, São Paulo, 127pp.

Miranda, L.B., 1982. Análise de massas de água da plataforma continental e da região oceânica adjacente: Cabo de São Tomé (RJ) a Ilha de São Sebastião (SP). Professorship Thesis, IOUSP, São Paulo, 123pp.

Odebrecht, C., Garcia, V.M.T., 1997. Phytoplankton. In: Seeliger, U., Odebrecht, C., Castello, J.P. (Eds.), Subtropical Convergence Environments: the Coast and Sea in the Southwestern Atlantic. Springer, Berlin, Heidelberg, 308pp.

Olson, D.B., Podestá, G.P., Evans, R.H., Brown, O.B., 1988. Temporal variations in the separation of Brazil and Malvinas currents. Deep-Sea Research 35 (12), 1971–1990.

Peterson, R.G., Stramma, L., 1991. Upper-level circulation in the South Atlantic Ocean. Progress in Oceanography 26, 1–73.

Piccolo, M.C., 1998. Oceanography of the Western South Atlantic continental shelf from 33 to 55°S. In: Robinson, A.R., Brink, K.H. (Eds.), The Sea, Vol. 11. Wiley, New York.

Piola, A.R., Rivas, A.L., 1997. Corrientes en la plataforma continental. In: Boschi, E.E. (Ed.), El mar argentino y sus recursos pesqueros, Tomo 1, Antecendentes históricos de las exploraciones en el mar y las características ambientales. INIDEP, Secretaría de Agricultura, Ganadería, Pesca y Alimentación, Mar del Plata, Argentina.

Piola, A.R., Campos, E.J.D., Möller Jr., O.O., Charo, M., Martinez, C., 2000. Subtropical Shelf Front off eastern South America. Journal of Geophysical Research 105, 6565–6578.

Press, W.H., Teukolsky, S.A., Vetterling, W.T., Flannery, B.P., 1992. Numerical Recipes in Fortran 77: the Art of Scientific Computing, Vol. 1. Fortran numerical recipes. Cambridge University Press, Cambridge, UK, 933pp.

Reid, J.L., Nowlin Jr., W.D., Patzerd, W.C., 1977. On the characteristics and circulation of the Southwestern Atlantic Ocean. Journal of Physical Oceanography 7, 62–91.

Schäfer, H., Krauss, W., 1995. Eddy statistics in the South Atlantic as derived from drifters drogued at 100 m. Journal of Marine Research 53, 403–431.

Silva Jr., C.L., Kampel, M., Araujo, C.E.S., Stech, J.L., 1996. Observação da penetração do ramo costeiro da Corrente das Malvinas na costa sul-sudeste do Brasil a partir de imagens AVHRR. In: Proceeding of the Eighth Brazilian Symposium on Remote Sensing, Salvador, Brazil.

Souza, R.B., 2000. Satellite and Lagrangian observations of mesoscale surface processes in the Southwestern Atlantic Ocean. Ph.D. Thesis, University of Southampton, Southampton, UK, 239pp.

Souza, R.B., Robinson, I.S., 1998. Lagrangian and infrared observations of surface currents in the Brazil–Malvinas Confluence Zone, 1993–1994. International WOCE Newsletter 31, 32–35 (Unpublished manuscript).

Stech, J.L., Lorenzzetti, J.A., 1992. The response of the South Brazil Bight to the passage of wintertime cold fronts. Journal of Geophysical Research 97 (C6), 9507–9520.

Stevenson, M.R., 1996. Recirculation of the Brazil Current South of 23°S. International WOCE Newsletter 22, 30–32 (Unpublished manuscript).

Stevenson, M.R., Souza, R.B., 1994. Recirculation of the Brazil Current South of 20°S. In: Abstracts from the Symposium: the South Atlantic—Present and Past Circulation, Bremen, Germany, 1994, Vol. 52. Berichte, Fachbereich Geowissenschaften, Universitat Bremen, p. 149.

Stevenson, M.R., Dias-Brito, D., Stech, J.L., Kampel, M., 1998. How do cold water biota arrive in a tropical bay near Rio de Janeiro, Brazil? Continental Shelf Research 18, 1595–1612.

Stramma, L., England, M., 1999. On the water masses and mean circulation of the South Atlantic Ocean. Journal of Geophysical Research 104 (C9), 20863–20883.

Sunyé, P.S. 1999. Effet de la variabilité climatique régionale sur la pêche de la sardinelle le long de la côte sud-est du Brésil (1964–1993). Ph.D. Thesis, Institut Universitaire Européen de la Mer, Université de Bretagne Occidentale, 130pp.

Sverdrup, H.U., Johnson, M.W., Fleming, R.H., 1942. The Oceans: their Physics, Chemistry and General Biology. Prentice-Hall, Englewood Cliff, NJ, 1087pp.

Sybrandy, A.L., Niiler, P.P., 1991. The WOCE/TOGA Lagrangian drifter construction manual. SOI Ref. 91/6, WOCE Report 63, 58pp.

Thomsen, H., 1962. Masas de agua caracteristicas del Oceano Atlantico parte Sudoeste. Publication H632, Secretaria de Marina, Servicio de Hidrografia Naval, Buenos Aires, 22pp.

Zavialov, P.O., Möller, O.O., 2000. Modeling and observations of currents off Southern Brazil and Uruguay: the Rio Grande Current. In: Zatsepin, A.G. (Ed.), Oceanic Fronts and Related Phenomena (Proceedings of the Fedorov International Memorial Symposium). IOC Workshop Report No. 159, UNESCO, GEOS, Moscow, pp. 612–617.

Zavialov, P.O., Ghisolfi, R.D., Garcia, C.A.E., 1998. An inverse model for seasonal circulation over the Southern Brazilian Shelf: near-surface velocity from the heat budget. Journal of Physical Oceanography 28, 545–562.

Zavialov, P.O., Wainer, I., Absy, J.M., 1999. Sea surface temperature variability off southern Brazil and Uruguay as revealed from historical data since 1854. Journal of Geophysical Research 104 (C9), 21021–21032.

Zavialov, P., Möller Jr., O., Campos, E., 2002. First direct measurements of currents on the continental shelf of Southern Brazil. Continental Shelf Research 22, 1975–1986.